STATIC AND DYNAMIC NONLINEAR ANALYSIS OF SEMI-RIGID STEEL FRAMES WITH NEW BEAM-COLUMN ELEMENT

M. Rezaiee-Pajand*, M. Bambaeechee and S.R. Sarafrazi

Department of Civil Engineering, Ferdowsi University of Mashhad
Mashhad, Iran
mrpajand@yahoo.com, mohsen_bambaeechee@yahoo.com, srsarafrazi@yahoo.com

*Corresponding Author

(Received: June 06, 2010 – Accepted in Revised Form: September 15, 2011)

***doi**: 10.5829/idosi.ije.2011.24.03a.01*

Abstract One of the important issues in the study of steel frames is to find a suitable formulation for semi-rigid connections. In this paper, the explicit stiffness matrix for a two-dimensional beam-column element having end-flexibilities is derived. The effects of the lateral uniformly distributed load on the deflection are considered. Both the tensile and compressive axial loads are also taken into account by one formula. Using the proposed stiffness matrix, some first-order, second-order, buckling, and dynamic analyses for semi-rigid frames are performed. The plastic analysis is also carried out using the plastic hinge approach. Comparing the calculated results with other references shows the accuracy and capabilities of the utilized element. Furthermore, the influences of the semi-rigid connections on the static and dynamic responses are investigated.

Keywords Dynamic Analysis, Beam-Column Element, Semi-Rigid Connection, Buckling Analysis, Plane Steel Frame, Plastic Analysis, Stiffness Matrix, Second-Order Effects

چکیده یک کارمهم پژوهشی درقاب های فولادی، رابطه سازی مناسب برای پیوند های نیمه-سخت است. در این مقاله، ماتریس سختی صریح یک جزء مستوی تیر- ستون با دو سر نرم برپا می شود. واردکردن هردو نیروی محوری کششی وفشاری در رابطه ی نویسندگان امکان پذیر است. با ماتریس سختی پیشنهادی، تحلیل های مرتبه ی یکم، مرتبه ی دوم، پایداری و پویا برای قاب های نیمه-سخت انجام می پذیرد. همچنین، تحلیل مومسان به وسیله ی راهکار مفصل مومسان به انجام می رسد. با مقایسه ی نتیجه ها با پاسخ های دیگر منبع ها، دقت ونیزکارایی جزء آشکار خواهد شد. افزون بر این، اثر پیوند های نیمه-سخت بر روی پاسخ های ایستا و پویای سازه بررسی می شوند.

1. INTRODUCTION

The analysis and design of the steel frames is usually carried out considering the rigid or pinned connections. Utilizing the rigid or pinned model is simple. However, these connections do not show the actual behavior of the structural joints. The experimental tests indicate that all connections are flexible through the loading process [1]. Therefore, the effect of connection behavior in the analysis must be considered. Accordingly, various investigations have been done on this topic so far. Some researchers have concentrated their attempts on the experimental studies [1, 2]. Hasan, et al. [3] classified the semi-rigid connections. Investigating the behaviors of the semi-rigid connections, and proposing new models are the other topic for research [4,5]. Many researchers have studied the analysis and design of the steel frames with semi-rigid connection [6-10] and others have worked on the design and optimization of these structures [11-13]. The results of all studies show that the connection flexibility has the appreciable influence on the structural responses, and it cannot be ignored. It should be noted that many Codes take into account the semi-rigid connections and semi-

rigid steel frames [14-16].

Heretofore, several finite elements have been proposed for analyzing the frames, which have semi-rigid connections. Chen and Lui presented some methods for analyzing semi-rigid frames [17]. They adopted rational stiffness values of the ends' connections for developing the stiffness matrix. Using the concept of self-equilibrating element, Zhou and Chan obtained a new element [17]. This element uses a fifth-order polynomial function for deflection and its stiffness matrix includes the effects of axial force and the stiffness of the ends' connections. Utilizing the end-fixity factor in turn of directly applying the value of connection stiffness, Xu presented an element to simplify the second-order analysis of steel frames [18]. Moreover, Sekulovic and Salatic used the exact stability functions and proposed an element which considered the second-order influences of the axial force and bowing effect [19]. Recently, Ihaddoudène et al. presented a model of the connection using three springs [6]. The second-order effects of the axial force were neglected by these investigators, and the plastic analysis was performed. Using the proposed element, Ihaddoudène et al. studied the forming of the plastic hinges. Also Liu et al. [7, 20, 21] investigated the inelasticity behavior of the structures with semi-rigid connections.

In the present work, a new beam-column element with semi-rigid connections is proposed. This element is very general and models a frame member with any type of connections. Furthermore, the members of the stiffness matrix are proposed with the closed-form expressions which have adequate accuracy. It is worth emphasizing that the new element has a single formulation for both the tensile and compressive axial forces. The influences of the uniformly distributed loads on the deformation of the member are also considered in the developed element. Moreover, it has been utilized for comparing the responses of steel framing in different types of analysis having various end-fixity factors. Static and dynamic analysis of several benchmark problems certifies the validity and efficiency of the proposed formulation. These analyses consist of the first-order, P-delta, buckling, and plastic behaviors. Furthermore, the numerical results are used to study the effects of connection flexibility on the responses of steel frames.

2. THE PROPOSED FORMULATION

Considering special effect in the structural analysis requires a proper formulation and suitable element. The major target of the present work is to take into account the connection flexibility and second-order effects in analyzing the plane steel frames. Consequently, a new beam-column element is utilized. Figure 1 shows the element specifications and the external load. The lateral load does not produce any torsion. The shear and warping deformations are also neglected. It should be emphasized that the rotational deformation is the only behavior which is considered for the beam to column connections. In other words, the axial and shear deformations in the connections are ignored. The connection flexibilities are simulated by two rotational springs. The rigidity of these springs is denoted by R_i and R_j. The moment-rotation relation of the spring could be linear, multi-linear or perfectly plastic. In the plastic analysis, only the bending moment is considered and the effects of axial forces are also neglected. Furthermore, the size of connection, in comparison to the columns and beams dimensions is ignored.

In the proposed element, a fifth-order polynomial describes the elastic deformation of the element as presented in Equation 1. Chan and Zhou used this function to obtain a semi-rigid element. It should be noticed that Chan and Zhou's formulation excluded the effects of the uniformly distributed load on the structural deflections [17].

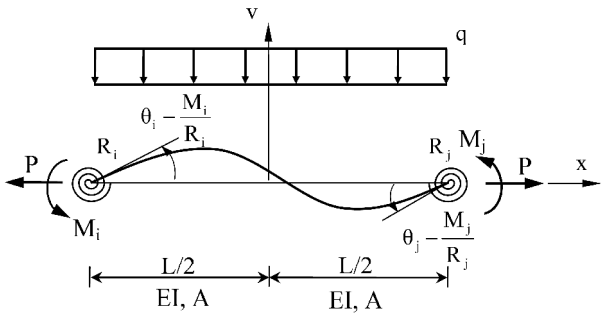

Figure 1. The semi-rigid 2D element in the basic axis.

$$v(x) = a_0 + a_1 x + a_2 x^2 + a_3 x^3 + a_4 x^4 + a_5 x^5 \ , \ -L/2 \le x \le L/2 \quad (1)$$

The parameter v shows the lateral displacement which is measured according to the straight line between the two end points. Satisfying the compatibility and the equilibrium conditions, the unknown factors, a_i, are obtained. These factors are presented in Appendix A. The compatibility conditions of the deformations are written at the two boundaries of the element as below:

$$(v)_{x=-L/2} = 0 \quad (2)$$

$$\left(\frac{dv}{dx}\right)_{x=-L/2} = \theta_i - \frac{M_i}{R_i} \quad (3)$$

$$(v)_{x=L/2} = 0 \quad (4)$$

$$\left(\frac{dv}{dx}\right)_{x=L/2} = \theta_j - \frac{M_j}{R_j} \quad (5)$$

Furthermore, the moment and shear equilibrium equations at the middle point of the element could be respectively written as follows:

$$EI\left(\frac{d^2v}{dx^2}\right)_{x=0} = \frac{M_j - M_i}{2} + \frac{qL^2}{8} + Pv \quad (6)$$

$$EI\left(\frac{d^3v}{dx^3}\right)_{x=0} = \frac{M_i + M_j}{L} + P\left(\frac{dv}{dx}\right)_{x=0} \quad (7)$$

As shown in Figure 1, the parameters M_i and M_j are respectively the internal bending moments of joints, i and j .The axial force is denoted by P. It is reminded that the lateral loads enforce no torsion, and they are assumed to be distributed across the element. The value of these loads per unit length of the member is q. The Equations 2 to 7 can be solved simultaneously and unknown factors can be found. Afterward, the secant stiffness equations are obtained using the energy method. To achieve this goal, the total potential energy function of the element, Π, is calculated using the following relations:

$$\Pi = U + V \quad (8)$$

$$U = \int_V \int_\varepsilon \sigma \, d\varepsilon \, dV \quad (9)$$

$$V = -(M_i\theta_i + M_j\theta_j + Pe + \int_L q(x)\, v(x)\, dx) \quad (10)$$

where, U and V are the strain energy and the external work, respectively. The axial deformation is also denoted by e. Minimizing the total potential energy and neglecting the axial elongation due to the bowing effect, the secant stiffness relationships for the proposed element are obtained as below:

$$\begin{Bmatrix} P \\ M_i - S_{13}(qL^2) \\ M_j + S_{23}(qL^2) \end{Bmatrix} = \frac{EI}{L}\begin{bmatrix} \frac{A}{I} & 0 & 0 \\ 0 & S_{11} & S_{12} \\ 0 & S_{21} & S_{22} \end{bmatrix} \begin{Bmatrix} e \\ \theta_i \\ \theta_j \end{Bmatrix} \quad (11)$$

Before writing the matrix entries, some parameters are described. Primarily, the end-fixity factor is taken as $r_k = 1/(1+3EI/R_kL)$, which is considered to be the stiffness of the semi-rigid connection in the joint $k=i, j$ [22]. It is clear that for a rigid connection the stiffness is infinite and the rigidity factor becomes 1. On the other hand, the zero value for r_k describes a pinned connection, which has zero rotational stiffness. For a semi-rigid connection, the end-fixity factor changes between zero and one. Moreover, the dimensionless ratio, PL^2/EI, is marked by ρ. The other required parameters are written in the below form:

$$S_1 = (58982400 + 5898240\rho + 1411072\rho^2 /7 + 321536\rho^3/105 + 716\rho^4/35 + 2\rho^5/45)/(\rho+80)^2(\rho+48)^2$$

$$S_2 = (29491200 + 1474560\rho + 214016\rho^2 /7 + 30976\rho^3/105 + 10\rho^4/21 - \rho^5/126)/(\rho+80)^2(\rho+48)^2$$

$$S_3 = \frac{192 + 24\rho/5 + 11\rho^2/420}{(\rho+48)^2}$$

$$H = (3r_i + (1-r_i)S_1)(3r_j + (1-r_j)S_1) - (1-r_i)(1-r_j)S_2^2 \quad (12)$$

Now, the secant matrix entries, S_{ij} , are written as follow:

$$S_{11} = \frac{1}{H}(9r_ir_jS_1 + 3r_i(1-r_j)(S_1^2 - S_2^2))$$

$$S_{12} = S_{21} = \frac{1}{H}(9r_i r_j S_2)$$

$$S_{13} = \frac{1}{H}(9r_i r_j S_3 + 3r_i(1-r_j)(S_1+S_2)S_3)$$

$$S_{22} = \frac{1}{H}(9r_i r_j S_1 + 3r_j(1-r_i)(S_1^2 - S_2^2))$$

$$S_{23} = \frac{1}{H}(9r_i r_j S_3 + 3r_j(1-r_i)(S_1+S_2)S_3) \qquad (13)$$

The coefficients S_{11}, S_{12}, S_{21} and S_{22} are indeed the stability functions of the semi-rigid member. Figure 2 illustrates the curves of these coefficients versus the variations of the axial force for different values of the end-fixity factors. For simplicity, the end-fixity factors of the two ends of the element are considered the same in these figures. Consequently, the functions S_{11} and S_{22} are also the same. It should be reminded that the curves of secant stiffness, which are shown in Figure 2, are similar to the work of Zhou and Chan [17]. These researchers presented S_{ij} in terms of the non-dimensional axial force, PL^2/π^2EI, and the connection-stiffness-control parameter $\eta = r/(r+4EI/L)$.

Figure 2 shows that the values of S_{11} and S_{22} change from 0 to four when the connection stiffness increases from zero to infinite and the axial force is zero. In this case, the coefficients S_{12} and S_{21} also change in the range of 0-2. On the other hand, the critical compressive axial force is decreased if the connection stiffness decreases. According to Equation 11, the fixed-end moments are related to the coefficients S_{13} and S_{23} and also to the value of the distributed loads. In other words, the parameters S_{13} and S_{23} include the influence of the end-fixities and second-order effect of axial force on the fixed-end moments. The mentioned parameters are plotted in Figure 3.

As shown in Figure 3, the parameters S_{13} and S_{31} are in the 0-1/12 domain while the axial load is zero. Furthermore, the values of these coefficients change more rapidly, if the connection stiffness decreases. In common engineering practice, in addition to the fixed-end moments, the shear reactions are required for structural analysis. The suggested formulation does not require the explicit expressions of these forces. In other words, the fixed-end shears can be easily calculated utilizing

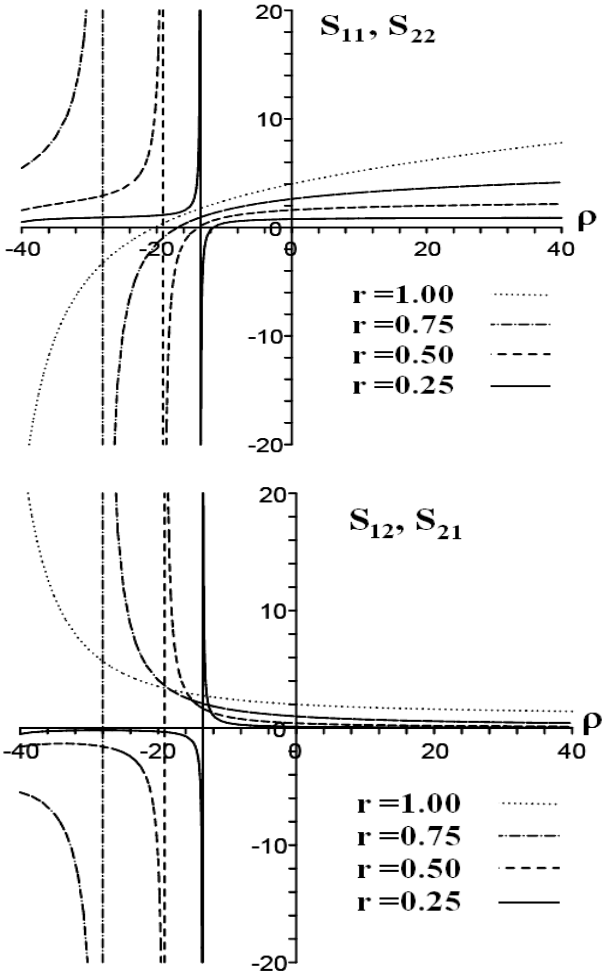

Figure 2. The curves of stability functions for different values of end-rigidities.

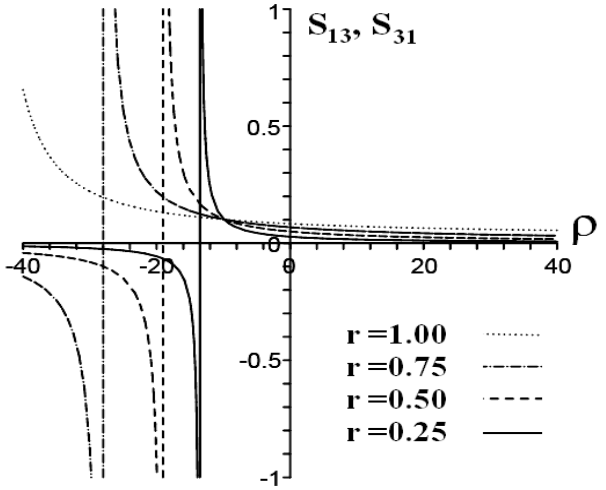

Figure 3. The curves of S_{13} and S_{31} functions for different values of end-rigidities.

the equilibrium equations.

It is worth emphasizing that the proposed stability functions have some errors near the critical axial load in comparison to the exact solutions. However, the developed relations are simpler than the exact ones and the errors are not significant. It is reminded that the exact stability functions are two sets of functions, which are presented separately for compressive and tensional axial forces. Another merit of this study is that, the effect of tension and compression loads are treated in the same way by the present formulation. The effects of any kind of loading and the geometric imperfections can be also modeled by the suggested scheme.

3. EXPLICIT STIFFNESS MATRIX

The stiffness matrix of a semi-rigid member in the basic axis was obtained in the previous section. According to Equation 11, this matrix has three relations between the element principal forces and their relative displacements. On the other hand, a general plane frame element has six degree of freedom, as shown in Figure 4. By performing some matrix operations, the secant stiffness of the mentioned element is obtained utilizing the entries of the matrix given by Equation 11. The compact result is presented in the below form:

$$\mathbf{p} = \mathbf{K}_{\mathrm{EL}}^{\mathrm{SR}}\mathbf{x} \tag{14}$$

In this equation, $\mathbf{K}_{EL}^{SR}$ is the stiffness matrix of the semi-rigid member in the local axis. The suggested matrix takes into account the second-order effects of the axial force and the connection flexibility. This matrix can be written in the below form:

$$\mathbf{K}_{\mathrm{EL}}^{\mathrm{SR}} = \frac{EI}{HL}\begin{bmatrix} K_{11} & 0 & 0 & K_{14} & 0 & 0 \\ & K_{22} & K_{23} & 0 & K_{25} & K_{26} \\ & & K_{33} & 0 & K_{35} & K_{36} \\ & & & K_{44} & 0 & 0 \\ & Sym. & & & K_{55} & K_{56} \\ & & & & & K_{66} \end{bmatrix} \tag{15}$$

Nonzero arrays of the stiffness matrix are given in Appendix B. The global stiffness matrix is easily obtained using the following transform matrix:

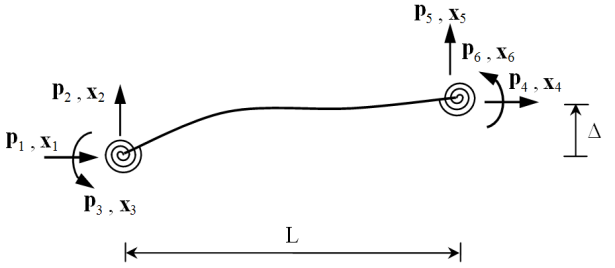

Figure 4. The six-DOF semi-rigid element.

$$\mathbf{K}_{\mathrm{EG}}^{\mathrm{SR}} = \mathbf{R}^{\mathrm{T}}\mathbf{K}_{\mathrm{EL}}^{\mathrm{SR}}\mathbf{R} \tag{16}$$

It is worth emphasizing that the obtained matrix can explicitly model a frame member with different types of connections. This element can be used in the second-order and buckling analysis of the steel frames as well. Furthermore, the stiffness formulation explicitly includes the effect of both tension and compression axial loads in a single relation. When the axial load is zero, Equation 15 changes to the required matrix for the first-order analysis of the semi-rigid frame. Furthermore, by setting the proper values for the end-fixity factors, the stiffness matrices of the truss or the common moment resistance frame elements are obtained. By utilizing this formulation, the special frame elements with different combination of rigid, pinned, semi-rigid connections for each end of the member are easily modeled. It is evident that the end-fixity factor is more important, since expresses the real condition of the connection.

4. THE BEHAVIOR OF CONNECTIONS

Commonly, the moment-rotation relationship describes the behavior of connections [23]. In the present investigation, it is assumed that the semi-rigid connections have a linear behavior. The basic equation for the linear model is defined as follows:

$$M = R\theta \tag{17}$$

In this equation, M is the moment and R and θ are the stiffness and rotation of the connection, respectively. The connection stiffness, R, could be considered as either the initial stiffness or the

secant connection stiffness. From this point on, except for the mentioned members, the connection stiffness is constant and equals to the initial secant stiffness. The multi-line and inelastic behaviors of connections are also considered in this paper. The inelastic behavior is assumed to be linear elastic and perfectly plastic.

5. DIFFERENT TYPES OF ANALYSIS

Several kinds of structural analysis are performed to show the abilities of the recommended element and also to study the effects of connection flexibilities on the structural responses. By neglecting the effects of the axial forces in the stiffness matrix, the first-order analysis of the semi-rigid frame is possible. On the other hand, the second-order analysis is carried out using the proposed stiffness matrix. It is reminded that the elements of the stiffness matrix in this case are affected by the values of the axial loads. Consequently, the P-delta analysis should be done by an iterative process up to the point of equilibrium state. The buckling loads of steel frames with semi-rigid connections could be also derived. The mentioned analysis is performed by evaluating the eigenvalues of the structural stiffness matrix. In other words, the external loads are incrementally increased until the lowest eigenvalue becomes zero or a negative value. The authors' experiences show that dividing the frame members into several elements has no appreciable effect on the response accuracy for the reason that the assumed function has the high order terms. To prove this merit, both examples in Section 7.3 were reanalyzed with more elements, and the same results were obtained.

The plastic behavior of the connection is also studied in the present paper. However, the second-order effects are neglected for this kind of analysis. While the multi-line relation is used for the plastic behavior, the Ihaddoudène algorithm could be applied for inelastic analysis of the structure [6]. The mentioned procedure pursues the sequence of the formation of the plastic hinges based on the moment-rotation function of connections. This procedure is a step by step precise process. For a general moment-rotation function, a common iterative tactic, such as dynamic relation method (DRM) or Newton-Raphson procedure should be utilized. Because the proposed element has an explicit stiffness matrix, the connection behavior does not increase the required time in the linear analysis. However, the nonlinear problems demand more computations to include connection effect. The details of dynamic analysis will be described in the next section.

6. DYNAMIC ANALYSIS

The dynamic analysis is performed by either the numerical time integration tactics or the modal analysis. Linear dynamic analysis is usually performed by the modal method. On the other hand, the numerical integration algorithms are more general and can be used for both linear and nonlinear system. In this kind of structural analysis, the total time interval is divided into finite steps. The dynamic equilibrium equations at the end of the n^{th} step are written in the below matrix form:

$$\mathbf{M}\ddot{\mathbf{X}}^{n+1} + \mathbf{C}^{n+1}\dot{\mathbf{X}}^{n+1} + \mathbf{K}^{n+1}\mathbf{X}^{n+1} = \mathbf{P}^{n+1} \tag{18}$$

where, $\mathbf{C}$ and $\mathbf{M}$ are damping and the mass matrices, and $\mathbf{P}$ is the applied force vector. The unknown parameters are displacements, velocities and the accelerations, which are shown by $\mathbf{X}$, $\dot{\mathbf{X}}$ and $\ddot{\mathbf{X}}$, respectively. Four numerical time integration tactic are utilized in the present study. They are the constant and linear acceleration algorithms of Newmark [24] Wilson-θ technique [25] and the 5th-order procedure of Rezaiee-Pajand and Alamatian [23]. These methods are denoted by NCA, NLA, WTM, IHOA-5, respectively. The mentioned methods calculate the velocities and the accelerations at time t_{n+1}, in terms of displacements at this time, and also the previous steps values. The extrapolations for the WTM, NCA and the NLA methods are written in the below generalized functions:

$$\begin{cases} \dot{\mathbf{X}}^{n+\theta} = \dfrac{\gamma}{\beta\,\theta\,\Delta t}(\mathbf{X}^{n+\theta} - \mathbf{X}^{n}) - (\dfrac{\gamma}{\beta} - 1)\dot{\mathbf{X}}^{n} - (\dfrac{\gamma}{2\beta} - 1)\,\ddot{\mathbf{X}}^{n}\,\theta\,\Delta t \\ \ddot{\mathbf{X}}^{n+\theta} = \dfrac{1}{\gamma\,\theta\,\Delta t}(\dot{\mathbf{X}}^{n+\theta} - \dot{\mathbf{X}}^{n}) - \dfrac{1-\gamma}{\gamma}\ddot{\mathbf{X}}^{n} \end{cases} \tag{19}$$

Technically, the WTM is a generalized process of the NLA, which evaluates the velocities and the accelerations at the extended time, $t_n+\theta\Delta t$. In special case, when the value of θ is 1, the WTM coincides with the NLA. The stability of the WTM depends on the time step. However, this is an unconditionally stable procedure, when the value of θ is greater than 1.37. The optimal value of θ is 1.42. Recently, Rezaiee-Pajand and Alamatian suggested a new higher-order time integration family. The 5th-order member of this family uses the following extrapolations:

$$\begin{cases} \dot{\mathbf{X}}^{n+1} = \frac{3325}{863\Delta t}(\mathbf{X}^{n+1}-\mathbf{X}^{n}) - \frac{2462}{863}\dot{\mathbf{X}}^{n} - \frac{487883}{414240}\Delta t\ddot{\mathbf{X}}^{n} \\ + \frac{163723}{103560}\Delta t\ddot{\mathbf{X}}^{n-1} - \frac{296671}{310680}\Delta t\ddot{\mathbf{X}}^{n-2} \\ + \frac{212963}{621360}\Delta t\ddot{\mathbf{X}}^{n-3} - \frac{3693}{69040}\Delta t\ddot{\mathbf{X}}^{n-4} \\ \ddot{\mathbf{X}}^{n+1} = (\frac{1440}{\Delta t}(\dot{\mathbf{X}}^{n+1}-\dot{\mathbf{X}}^{n}) - 1427\ddot{\mathbf{X}}^{n} + 798\ddot{\mathbf{X}}^{n-1} - \\ 482\ddot{\mathbf{X}}^{n-2} + 173\ddot{\mathbf{X}}^{n-3} - 27\ddot{\mathbf{X}}^{n-4})/475 \end{cases} \tag{20}$$

In the numerical time integration strategies, the acceleration and the velocity extrapolation vectors are substituted in the dynamic equilibrium equation. As a result, a system of equations in the terms of $\mathbf{X}^{n+1}$ is obtained, which has the below general form:

$$\begin{aligned} &(\frac{\xi}{\Delta t^2}\mathbf{M} + \frac{\eta}{\Delta t}\mathbf{C}^{n+1} + \mathbf{K}^{n+1})\mathbf{X}^{n+1} = \\ &\mathbf{P}^{n+1} - \mathbf{M}\mathbf{f}_1 - \mathbf{C}\mathbf{f}_2 \sim \mathbf{K}_{eq}\mathbf{X}^{n+1} = \mathbf{P}_{eq} \end{aligned} \tag{21}$$

where, ξ and η are the constant parameters and $\mathbf{f}_1$ and $\mathbf{f}_2$ are functions of the displacement, velocity and the acceleration vectors of step n and the accelerations of the previous ones. Starting from initial conditions, the right hand side of Equation 21 is known and the unknown variables are calculated step by step. In general case, Equation 21 is a nonlinear system of equation and should be solved using an iterative method. The Dynamic Relaxation method (DRM) is a simple and a powerful procedure to solve the linear and nonlinear equations. Because of this merit, the combination of the numerical time integration and the DRM, are utilized to solve dynamic problems [26].

7. NUMERICAL EXAMPLES

To show the robustness of the proposed element, some benchmark problems are analyzed and the solutions are compared with other references. Moreover, the effects of connection flexibility on behavior of the steel frame are investigated.

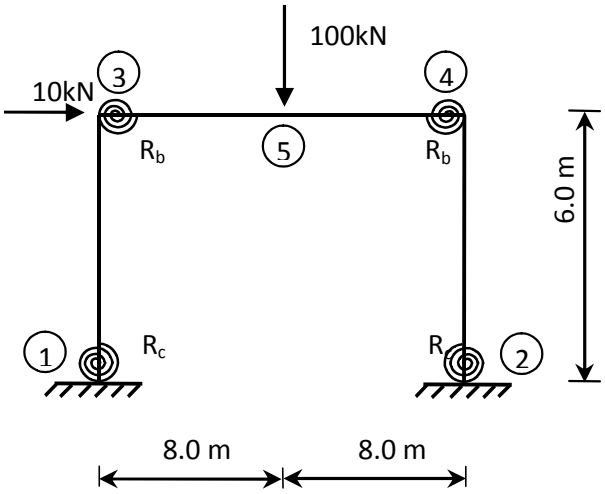

Figure 5. Portal frame with flexible connections.

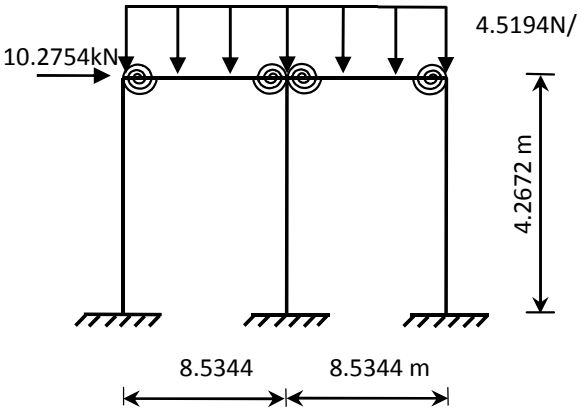

Figure 6. One-storey two-span frame.

7.1. First-Order Analysis The first-order analysis of two frames of Figures 5 and 6 are studied. The structures are loaded with the horizontal and vertical forces. At first, the portal frame of Figure 5 is considered. The section areas of the beam and its columns are respectively 76 cm^2 and 110 cm^2, and the corresponding moments of inertia are 21500 cm^4 and 9460 cm^4. The modulus of elasticity is assumed to be 205GPa. According to Table 1, a variety of connection stiffness values are considered for the beam to column and also for the base-plate connections. The absolute values of the internal moments at the end of the members are also computed and arranged in Table 1. The values in parentheses show the available solutions by other investigators [27]. The comparison between two groups of the results shows the accuracy of the proposed element for analysis of semi-rigid connections.

Figure 6 shows the one-storey two-span frame. The sections of the beams and columns are W21×57 and W10×22, respectively. The stiffness the beams to columns connections are 7.8807 kN.m/rad (45000 kip-in/rad). The elasticity modulus of the material is also 200GPa. The curves of the bending moment are plotted in Figure 7, for both rigid and semi-rigid connections. Chen studied this structure with semi-rigid connections [28]. The numbers in parentheses of Figure 7 are computed by Chen.

Figure 7 shows that the solutions of the new element are correct. Furthermore, the results of the

TABLE 1. The Absolute Values of Internal Moments (kN.m) for the frame of Figure 5.

Moments	Semi-Rigid Connections			Rigid Connections
	r_c=0.25, r_b=0.40 (R_c=EI_c/L_c,R_b=$4EI_b/L_b$)	r_c=1, r_b=0.40 (R_c=∞,R_b=$4EI_b/L_b$)	r_c=1, r_b=0 (R_c=∞,R_b=0)	r_c=1, r_b=1 (R_c=∞,R_b=∞)
M_{13}	0.32 (0.3)	31.67 (31.7)	30.04 (30)	52.23 (52.2)
M_{31}	80.25 (80.3)	93.65 (93.6)	0.00 (0)	127.50 (127.5)
M_{24}	24.16 (24.2)	71.53 (71.5)	29.96 (30)	87.14 (87.1)
M_{42}	116.41 (116.4)	113.80 (113.8)	0.00 (0)	152.59 (152.6)
M_{54}	301.67 (301.7)	296.28 (296.3)	400.00 (400)	260.00 (260.0)

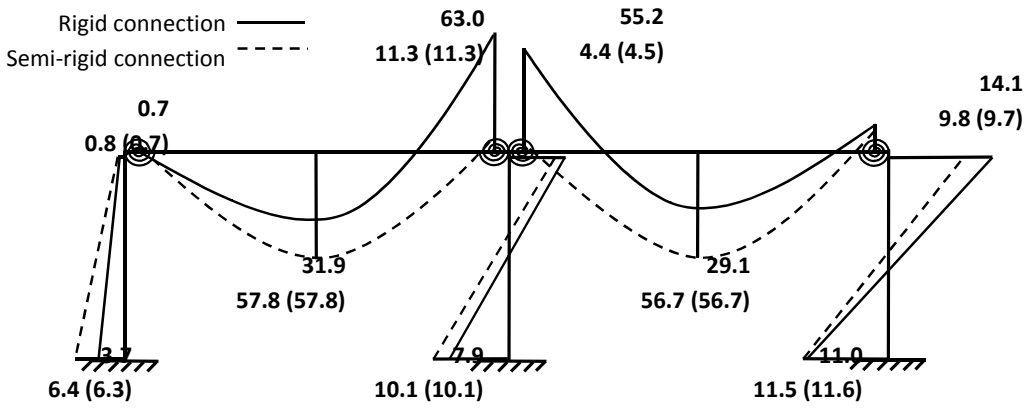

Figure 7. The bending moment diagrams (kN.m).

two problems demonstrate that the connection flexibility has a considerable effect on the frame internal force distributions.

7.2. Second-Order Analysis To prove the accuracy of the proposed stiffness matrix, a portal frame with flexible connections is analyzed. As shown in Figure 8, the mentioned structure is subjected to the nodal and distributed loads. The beam and columns of the frame are made of IPE22 and IPB14 sections, respectively. The value of the Yang's modulus is 210GPa.

The P-delta and the first-order analysis are performed for the four rigid, TSDWA, DWA and pinned beam to column connections. It should be reminded that the TSDWA connects the beam to column by employing top and seat angles with double web angles. Double web angles also construct the DWA connection. Based on the reference [19], the values of the rotational stiffness for the TSDWA and DWA connections are 11300 and 6100 kN.m/rad, respectively. The values of P=450kN and q=250kN/m are also selected for loads. Some of the results for displacements and moments are presented in Tables 2 and 3. The structural responses are compared with those obtained by Sekulovic and Salatic [19].

Tables 2 and 3 show that there is no substantial difference between the calculated results and those reported in reference [19]. It is reminded that Sekulovic and Salatic used the exact stability functions in terms of hyperbolic sine and cosine functions, whereas a fifth-order polynomial is utilized in the proposed method.

Consequently, the proposed stiffness matrix based on the fifth-order polynomial has a high accuracy. Moreover, changing the connection rigidities makes appreciable variations in the distribution of the internal loads and the nodal displacements. The second-order analysis also increases these changes. The variations of some selected solutions versus the rigidity of the beam to column connection are plotted in Figures 9 and 10, for the first-order analysis. Similar curves are also presented in Figures 11 and 12, for the second-order analysis. It should be noticed that the solutions are normalized based on the outcomes of using the rigid connections.

7.3. Buckling Analysis Two braced and un-braced semi-rigid frames, as shown in Figure 13, are selected to perform the buckling analysis utilizing the new element. The mentioned frames are studied by Raftoyiannis in 2005. This investigator applied the exact stability analysis to find the buckling loads [29]. In both structures, the sections IPE30, HEA24 and L60×6 are used for the beams, columns and braces, respectively. The modulus of the elasticity is 210GPa. In addition, the stiffness of the semi-rigid beam to column connections is assumed to be constant and equal to 75566.6085 kN.m/rad.

From Table 4, it is observed that the proposed method for computing the buckling load has an acceptable accuracy. It is reminded that Raftoyiannis used the exact stability functions. Furthermore, the critical load of stricter is reduced by decreasing of the connection flexibility. However, this effect is reduced in the braced frames. It should be added that only one of the braces is used to obtain the braced frame critical load. Showing the influence of connection flexibility on the value of the critical load, some buckling analyses are performed on the un-braced frame of Figure 13. The calculated responses are normalized by those achieved utilizing the rigid connections. The related curves are plotted in Figure 14. It can be observed that the variation of the critical load with respect to the end-fixity values is approximately linear. Moreover, when the rigidity of the connection increases, the slope of the curve is also increased.

7.4. The Plastic Analysis The rigidities of the connections are affected by the elasto-plastic behavior of a steel structure. Moreover, the sequence forming of the plastic hinges and also the ultimate external load are related to the stiffness of the connections. Verifying these properties, the portal steel frame of Figure 15 is analyzed. Based on the reference [6], all sections of this structure are IPE33.

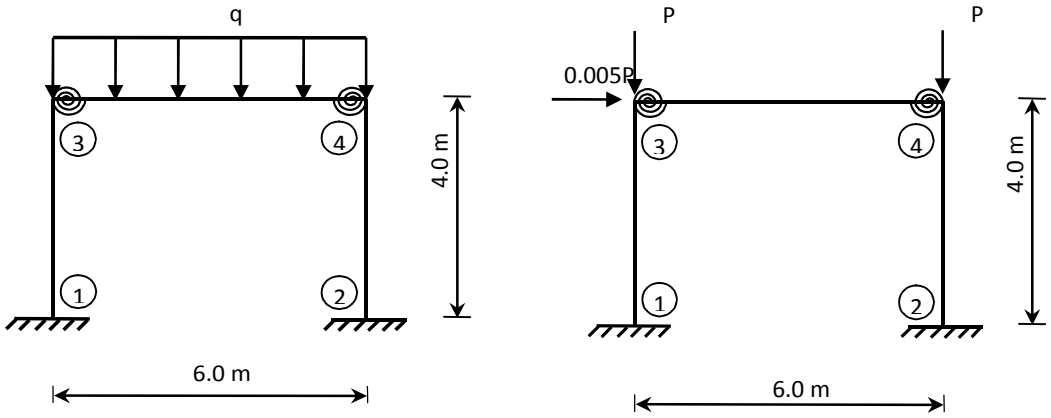

Figure 8. Simple portal frame.

TABLE 2. The Results of Applying the Nodal Loads

Outcome	Type of Connection	First-Order		Second-Order	
		Presented Study	Ref. [19]	Presented Study	Ref. [19]
Horizontal Displacement of Node 3($\times 10^{-4}$ m)	Pinned	75.72	75.73	936.31	936.21
	DWA	30.79	30.95	47.12	47.49
	TSDWA	28.96	28.70	42.97	42.39
	Rigid	25.79	25.79	36.42	36.42
Bending Moment Of Node 1 (kN. m)	Pinned	4.502	4.503	46.638	46.629
	DWA	2.722	2.728	3.890	3.908
	TSDWA	2.649	2.639	3.690	3.663
	Rigid	2.524	2.524	3.375	3.376

TABLE 3. The results of Applying the Distributed Load.

Outcome	Type of Connection	First-Order		Second-order	
		Presented Study	Ref. [19]	Presented Study	Ref. [19]
Rotation of Node 3($\times 10^{-3}$ Rad)	DWA	123.27	122.63	142.93	137.64
	TSDWA	131.54	132.81	152.13	149.83
	Rigid	146.91	146.94	166.84	166.46
Bending Moment of Node 1(kN. m)	DWA	194.87	193.69	242.19	233.08
	TSDWA	207.94	209.78	257.78	253.12
	Rigid	232.23	232.09	282.70	281.87

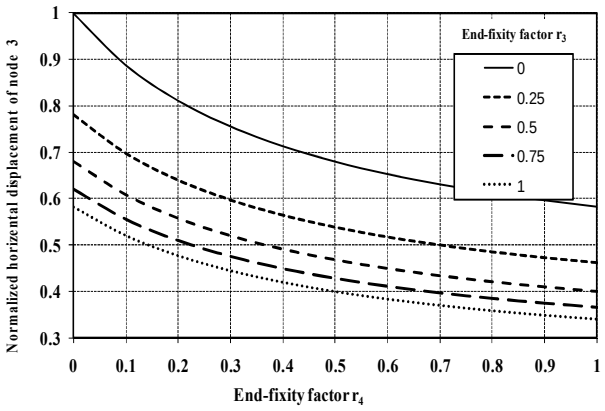

Figure 9. The influence of connection flexibility on the horizontal displacement in the first-order analysis.

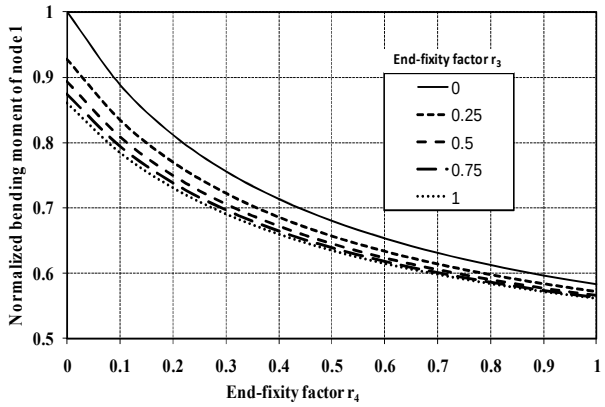

Figure 10. The influence of connection flexibility on the bending moment in the first-order analysis.

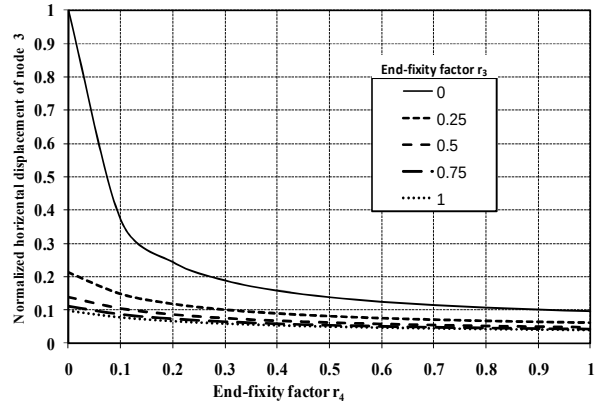

Figure 11. The influence of connection flexibility on the horizontal displacement in the second-order analysis.

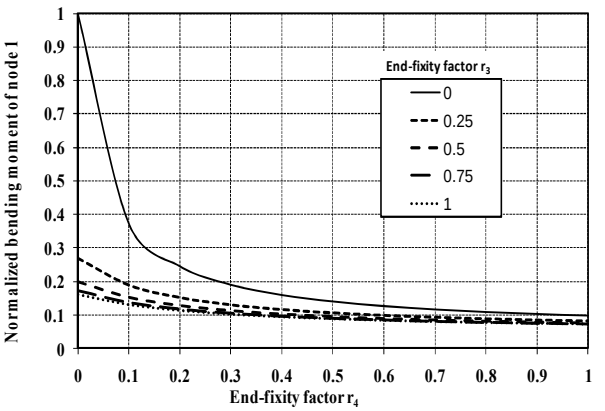

Figure 12. The influence of connection flexibility on the bending moment in the second-order analysis.

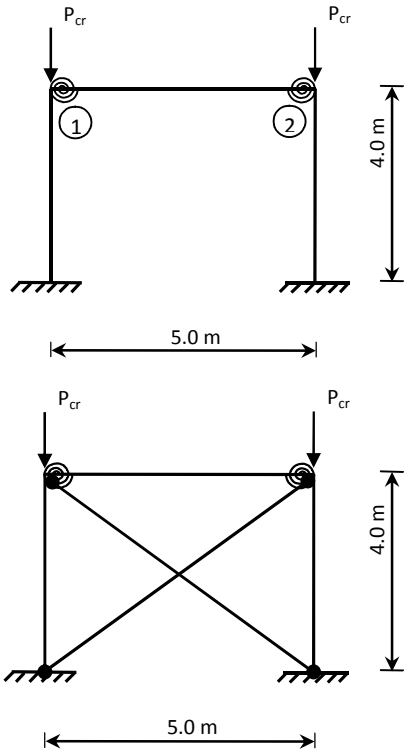

Figure 13. The braced and un-braced simple rectangular frames.

For the sake of comparison, the plastic moments of the joints and frame elements are considered $M_p^{joint} = 114.13$ kN.m and $M_p = 2S_x\sigma_e = 192.96$ kN.m, respectively.

Four cases of semi-rigid connections are considered for the mentioned frame. In the first case, all connections of 1 to 4 are semi-rigid. The

beam to columns and columns to base connections are rigid for respectively the second and the third cases, and the other connections remain semi-rigid. All connections of the final case are assumed to be rigid. Furthermore, four classes of the moment-rotation behavior for the semi-rigid connections are investigated, based on Figure 16.

The first set of analysis is performed for trilinear model of semi-rigid connections. The obtained ultimate load and the corresponding horizontal displacement of joint 2 and also the results of Ihaddoudène are arranged in Table 5. The presented solutions certify the accuracy of the proposed element.

TABLE 4. The Buckling Load of the Simple Rectangular Frame (kN).

Type of Connection	Un-braced, Fixed Support			Braced, Hinged Support		
	Presented Study Number of Element Per Member		Ref. [29]	Presented Study Number of Element Per Member		Ref. [29]
	1	4		1	4	
Pinned	2513	2513	2513	10060	10060	10052
Semi-rigid	4655	4656	4658	11659	11658	11647
Rigid	7227	7227	7244	12823	12823	12805

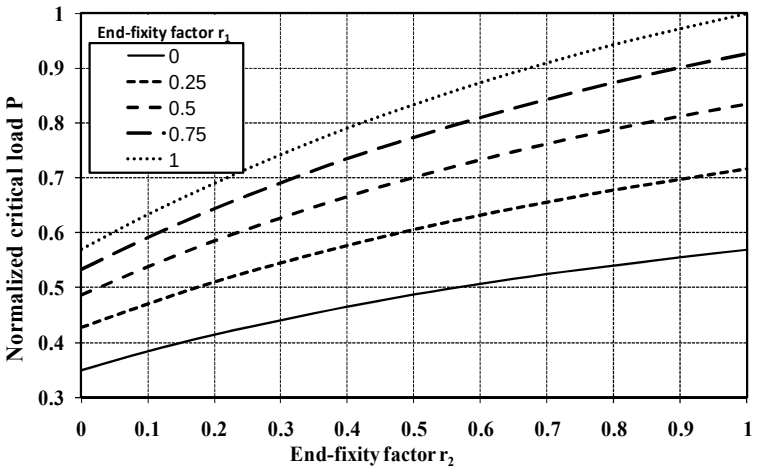

Figure 14. The influence of the connection flexibility on the critical load.

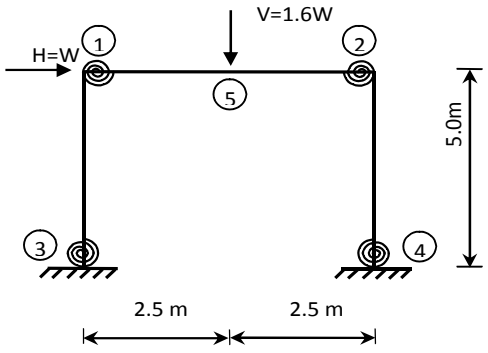

Figure 15. Portal frame

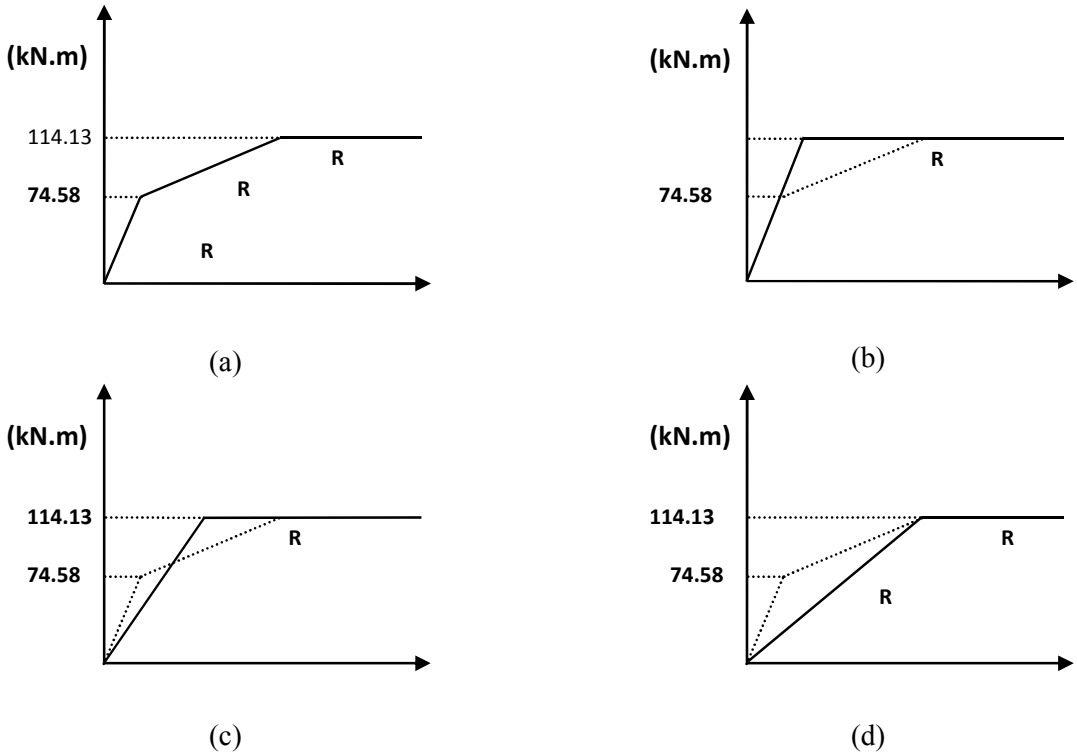

Figure 16. The moment-rotation models for semi-rigid connections, (a) Trilinear connection model (T1), (b) Bilinear connection model (B1), (c) Bilinear connection model (B2) and (d) Bilinear connection model (B3).

TABLE 5. The Results of the Trilinear Connection Model.

Type of Frame	Connections	Connections	Horizontal Displacement of Node 2 (m)		Failure Load (kN)	
			Presented Study	Ref. [6]	Presented Study	Ref. [6]
Case 1	Semi-rigid	Semi-rigid	0.0963	0.0957	91.3032	91.293
Case 2	Semi-rigid	Rigid	0.0953	---	111.1433	---
Case 3	Rigid	Semi-rigid	0.0555	0.0556	111.1213	111.122
Case 4	Rigid	Rigid	0.0539	0.0542	128.6388	128.640

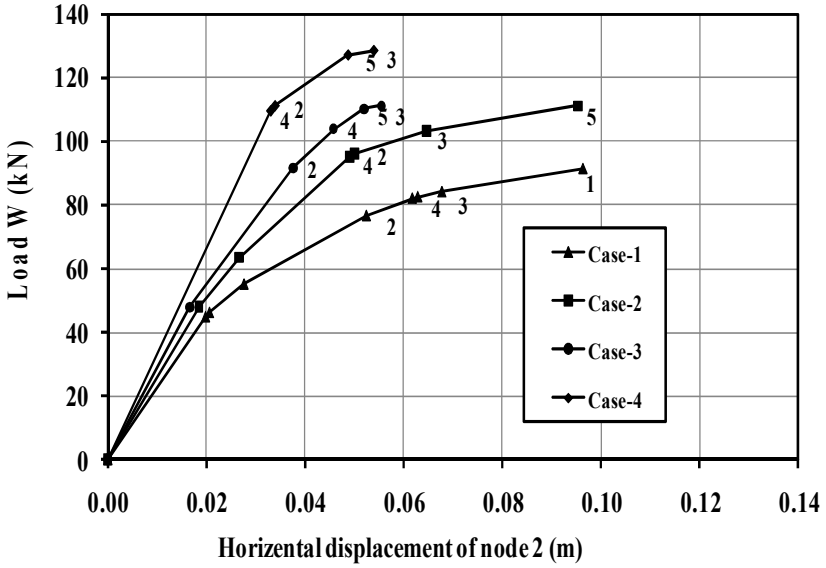

Figure 17. The load-displacement curves for the trilinear connection model.

TABLE 6. The Step-by Step Ihaddoudène Analysis for Case 1 and Trilinear Model of Connection.

step	$\Delta W^{(i)}$ (kN)	$\Delta M_1^{(i)}$ (kN.m)	$\Delta M_2^{(i)}$ (kN.m)	$\Delta M_3^{(i)}$ (kN.m)	$\Delta M_4^{(i)}$ (kN.m)	$\Delta M_5^{(i)}$ (kN.m)	$\Delta u_2^{(i)}$ (m)
1	44.8332	23.806	-74.580	-53.459	72.325	64.277	0.0198
2	1.3105	0.895	-1.290	-2.112	2.255	2.423	0.0008
3	8.8977	9.169	-9.218	-19.009	7.091	17.770	0.0070
4	21.5333	29.152	-29.042	-24.761	24.712	43.123	0.0248
5	5.4480	10.293	0.000	-9.198	7.747	16.043	0.0093
6	0.4640	1.265	0.000	-1.054	0.000	1.560	0.0011
7	1.5434	3.180	0.000	-4.537	0.000	4.677	0.0049
8	7.2731	36.370	0.000	0.000	0.000	32.731	0.0286
$\sum$	91.3032	114.13	-114.13	-114.13	114.13	182.604	0.0963

When the loads increase, the plastic hinges take form step by step at the points with extreme moments. Indeed, the values presented in Table 5 are related to the final state. Whereas, the effects of

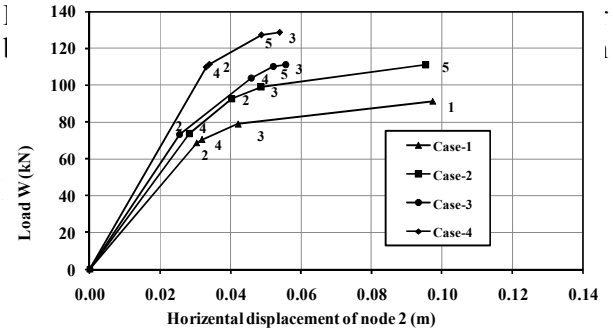

Figure 18. The load-displacement curves for the B1 bilinear connection model**.**

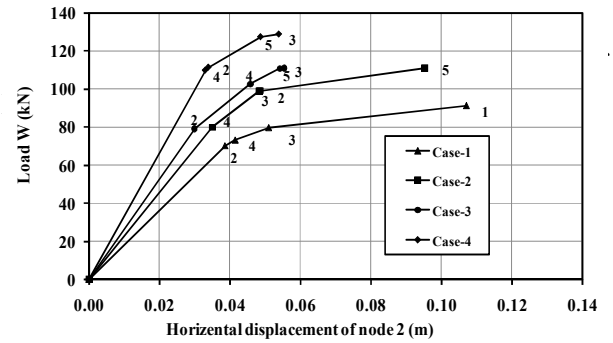

Figure 19. The load-displacement curves for the B2 bilinear connection model.

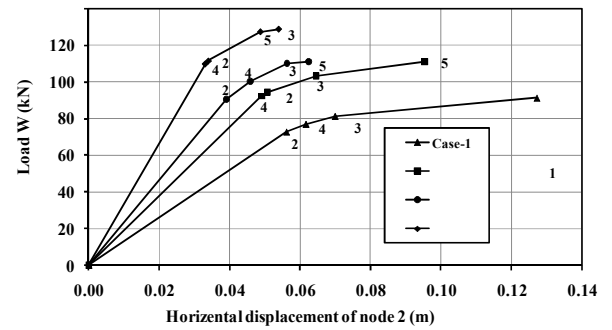

Figure 20. The load-displacement curves for the B3 connection model.

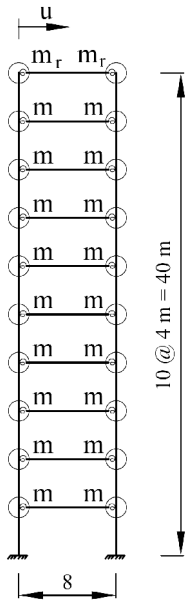

Figure 21. The 10-story frame.

7.5. Dynamic Analysis A one-span ten-story steel frame, which was studied by Sekulovic et al. [30], is selected for the first dynamic analysis. This structure is shown in Figure 21. No external forces are applied to this 10-story frame. The weight of structure is also zero. The masses of the frame concentrated at the nodal points are shown in Figure 21. The values of the m and m_r masses are 8000 and 6000 Kg, respectively. The modulus of elasticity for this system is 210 GPa. The properties of the sections for this structure are inserted in Table 7.

The mentioned structure is excited by the following ground acceleration:

$$\ddot{x}_g = \begin{cases} 0.2\,\text{m/s}^2 & 0 \le t \le 1\text{s} \\ 0.4\,\text{m/s}^2 & 1\text{s} \le t \le 3\text{s} \\ 0 & 3\text{s} \le t \end{cases}$$

The rigid, TSDWA and DWA beam-column connections are considered. It is reminded that the value of end-rigidities for the TSDWA and DWA connections are assumed as 0.795 and 0.6765, respectively. The value of 0.01 second is selected for the time step and the NCA and WTM time integration processes are utilized to analyze the structure. The time-displacement curves for the index displacement, *u*, are plotted in Figure 22. It should be noted that the results of these two methods are the same. Furthermore, the accuracies of the responses are checked using the NLA and also the IHOA-5 tactics, when the value of the time step is equal to 0.0005 s.

The response of the mentioned structure with rigid connections was presented by Sekulovic et al. [30], which is the same as the corresponding curve of Figure 22. The other curves show the influence of end-fixities on the responses of the structure. The reduction of the connection rigidities causes the appreciable growth of the response magnitudes, especially when the structure oscillates freely. Figure 23 shows the other moment resistant steel frame which is analyzed dynamically. The structure is loaded by the uniform gravity and the lateral wind forces. The value of gravity loads at the roof story and the other stories are 59.45 and 74.14 kN/m, respectively. The sections and the material properties of this structure are shown in Table 8.

It should be reminded that this structure was used by Morris et al. [31] for studying the effect of semi-rigid connections. Further, Xu analyzed it and investigated the effect of P-delta effect [18]. Verifying the validity of the proposed element, three end-rigidity factors, such as 1, 0.8 and 0.5, are considered for beams in the present work. Some linear and second-order analyses are performed and the horizontal displacements of the middle-top node of building, *u*, are arranged in Table 9. It is worth emphasizing that the present solutions are the same as those obtained by Xu.

In the second part, the merit of the new element for dynamic analysis is investigated. Consequently,

TABLE 7. The section Properties of the 10-Story Frame.

Section	member	stories	A (m^2)	I (m^4)
C1	column	1-4	0.027	1.71×10^{-3}
C2	column	5-7	0.0218	7.989×10^{-4}
C3	column	8-10	0.0149	2.517×10^{-4}
B	beam	all	0.306	2.569×10^{-3}

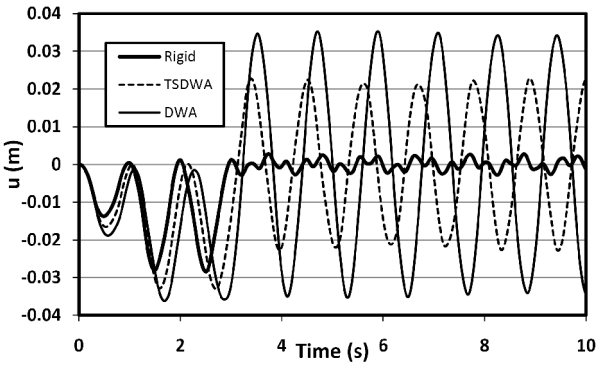

Figure 22. Time-displacement curve for 10-story frame.

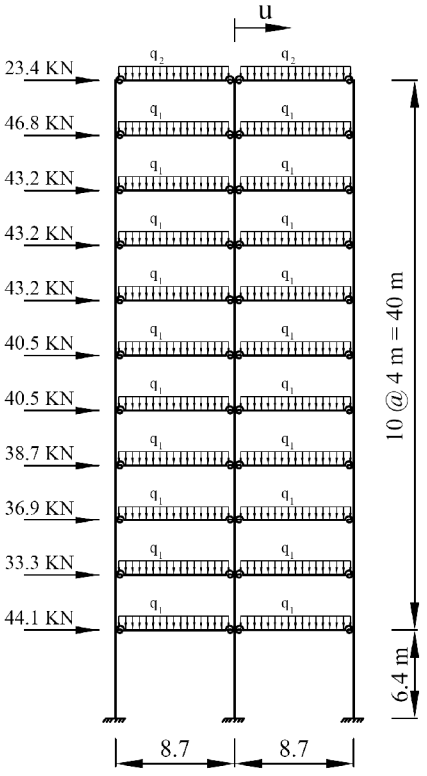

Figure 23. The 11-story structure.

the gravity loads are assumed to be constants and the horizontal forces are applied during ten second. In other words, the equivalent wind loads are zero at the beginning time. They are increased linearly until they reach the values of Figure 23 at 10 second. After that, they are constants. Some lumped masses are also added to the joints and the weights of the members are ignored. The concentrated masses for the middle and outer joints of the roof are 52000 and 26000 kg, respectively. The similar values for the other stories are 66000 and 33000 kg, respectively.

The first and also second-order dynamic analyses are performed for the 11-story structure using the WTM, NCA methods and $\Delta t = 0.1s$. The results are verified by utilizing the NLA and IHOA-5 process, with $\Delta t = 0.005$ and 0.002 seconds, respectively. The curve of the indicative drifts of the structure, *u*, are presented in Figure 24 for the aforementioned values of end-rigidity factors.

As shown in Figure 24, the lateral displacements are increased when the end-rigidity factors of beams are decreased. Therefore, the second-order effects on the drifts of structure become appreciable. Moreover, the declines in the connection rigidity intensify the response amplitudes. In addition, the periods of solutions increase if the values of the end-fixities decrease. The P-delta effects for this frame also increase the period of solutions.

TABLE 8. The Properties of Sections and Materials.

Section	member	stories	A (mm^2)	I (mm^4)	E (GPa)
C1	column	1-2	52200	1.89×10^9	200
C2	column	3-4	35000	1.3×10^9	
C3	column	5-6	34800	1×10^9	
C4	column	7-8	31000	8.94×10^8	
C5	column	9-11	22700	6.86×10^8	
B	beam	all	15700	7.61×10^8	

TABLE 9. The Middle-Top Node Displacements.

Rigidity Factor	Displacement , u (mm)	
	Linear Analysis	Second-Order Analysis
1	126	140
0.8	168	196
0.5	286	377

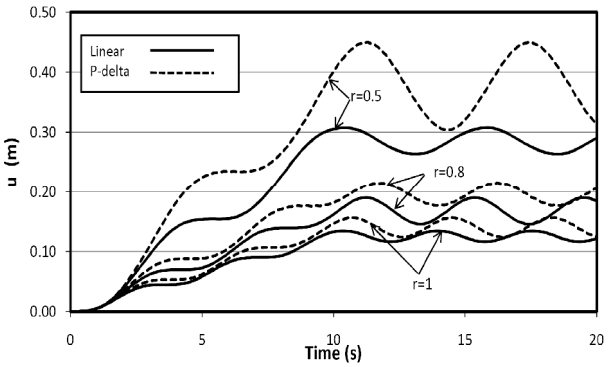

Figure 24. The curves of the parameter *u* for different values of the end-rigidity.

8. CONCLUSIONS

At first, a new formulation for the second-order elastic analysis of the plane steel frame was employed. The suggested element has semi-rigid connections and can take the nodal and uniformly distributed loads. The developed stiffness matrix can model the tensile and compressive members with one formulation, whereas the other researchers use different relations for comparison and tension. Moreover, the exact solutions which are in terms of hyperbolic sine and cosine functions are approximated employing a fifth-order interpolation. In addition, the stiffness matrix has a closed form. Consequently, the solution accuracy is preserved and the analysis duration decrease and the element become efficient. It should be noted that the proposed stiffness matrix is very general and can be utilized in the analysis of the frame member with different types of connections. Accordingly, the responses of steel framing with adoption of various end-fixity factors are accessible. The developed element is also suitable for dynamic analysis. Both linear and nonlinear frame analysis can be performed by this element.

In the second part of the paper, several first-orders, P-delta, buckling, plastic and dynamic analyses are performed using the benchmark semi-rigid structures. The comparisons of the solutions with those obtained by other researchers certify the high accuracy and capabilities of the employed element. In addition, the effects of connection flexibility on the responses of structures are studied. From the numerical solution point of view, the following results are concluded:

1. Changing the connection rigidities makes appreciable variations in the distribution of the internal loads and the nodal displacements. The second-order effects and non-linear behavior of connection also intensify these variations.
2. The connection flexibility reduces the structural critical load. However, this effect in the braced frames is lower than the un-braced one. The variation of the critical load with respect to the end-fixity values is approximately linear.
3. The sequence formation of the plastic hinges in frames, and their failure points depend on the connection flexibility and the corresponding moment-rotation curve. Among the different places of the connection, the foundation connections have more effect on the collapse point of structure. On the other hand, the flexibilities of the beam to column connections have little influence on the ultimate drifts and only decrease the fracture load. Moreover, the ultimate loads of the frames are independent of the moment-rotation model of the connection and are only depended on the moment capacity of the connections or members.
4. The outcomes of dynamic analysis show that the reduction of the connection rigidities softens the structure. Consequently, the magnitude and period of structural vibration are appreciably increased, which intensify the lateral displacements and also the second-order effects of axial loads. It should be added that the P-delta effects also increase the period of structure.

9. NOMENCLATURE

$\mathbf{K}$ =	stiffness matrix
$\mathbf{P}$=	force vector
$\mathbf{R}$=	transformation matrix
$\mathbf{M}$=	mass matrix
$\mathbf{C}$=	damping matrix
$\mathbf{X}$, $\dot{\mathbf{X}}$, $\ddot{\mathbf{X}}$=	displacement, velocity and acceleration vectors
R, r=	rotational stiffness value and end-fixity factor
M, P=	internal moment and axial force
S_{ij} =	stability functions of the semi-rigid connection

10. APPENDIX

10.1. Appendix A Coefficients of interpolation function

The factors of the interpolation function, which is defined in Equation 1, are derived as below:

$$a_0 = \frac{6}{(\rho+48)}(L\theta_i - L\theta_j) - \frac{qL^4}{8EI(\rho+48)}$$

$$a_1 = \frac{-20}{\rho+80}(L\theta_i + L\theta_j)$$

$$a_2 = \frac{\rho-48}{2(\rho+48)}(L\theta_i - L\theta_j) + \frac{qL^4}{EI(\rho+48)}$$

$$a_3 = \frac{1}{20}(\rho-80)a_1$$

$$a_4 = \frac{-2\rho}{(\rho+48)}(L\theta_i - L\theta_j) - \frac{2qL^4}{EI(\rho+48)}$$

$$a_5 = -\frac{1}{5}(\rho)a_1$$

10.2. Appendix B Nonzero terms of the stiffness matrix

The parameters of the stiffness matrix, which is used in Equation 13, are defined as below:

$$K_{11} = K_{44} = -K_{14} = AH/I$$

$$K_{22} =$$

$$K_{55} = [3(S_1 + S_2)\{6r_i r_j + (r_i + r_j - 2r_i r_j)(S_1 - S_2)\} + \rho] / L^2$$

$$K_{23} = -K_{25} = -K_{35} =$$
$$3\, r_i (S_1 + S_2)\{3r_j + (1 - r_j)(S_1 - S_2)\} / L$$

$$K_{26} = -K_{56} =$$
$$3r_j (S_1 + S_2)\{3r_i + (1 - r_i)(S_1 - S_2)\} / L$$

$$K_{33} = 9r_i r_j S_1 + r_i (1 - r_j)(S_1^2 - S_2^2)$$

$$K_{36} = 9r_i r_j S_2$$

$$K_{66} = 9r_i r_j S_1 + r_j (1 - r_i)(S_1^2 - S_2^2)$$

11. REFERENCES

1. Yang, C.M. and Kim, Y.M., "Cyclic Behavior of Bolted and Welded Beam-to-Column Joints", ***Int. J. Mech. Sci***., Vol. 49, (2007), 635-649.
2. Iványi, M., "Full-scale tests of steel frames with semi-rigid connections, ***Eng. Struct***., Vol. 22, (2000), 168-179.
3. Hasan, R., Kishi, N. and Chen, W.F., "A new nonlinear connections classification system", ***J. Constr Steel Res***., Vol. 47, (1998), 119-140.
4. Pirmoz, A., Khoei, A.S., Mohammadrezapour, E. and Daryan, A.S., "Moment–rotation behavior of bolted top–seat angle connections", ***J. Constr Steel Res***., Vol. 65, (2009), 973-984.
5. Mohamadi-shooreh, M.R. and Mofid, M., "Parametric analyses on the initial stiffness of flush end-plate splice connections using FEM", ***J. Constr Steel Res***., Vol.64 (2008) 1129-1141.
6. Ihaddoudène, A.N.T., Saidani, M. and Chemrouk, M., "Mechanical model for the analysis of steel frames with semi rigid joints", ***J. Constr Steel Res***., Vol. 65, (2009), 631-640.
7. Liu, Y. Xu, L. and Grierson, D.E., "Inelastic analysis of semirigid frameworks, in: Advances in Engineering Structures", Mechanics and Construction, Springer Netherlands, (2006), 317-328.
8. Aristizabal-Ochoa, J.D., "Slope-deflection equations for stability and second-order analysis of Timoshenko beam–column structures with semi-rigid connection", ***Eng. Struct***., Vol. 30 (2008), 2517–2527.
9. Silva, J.G.S., Lima, L.R.O., Vellasco, P.C.G., Andrade, S.A.L. and Andrade, R.A., "Nonlinear dynamic analysis of steel portal frames with semi-rigid connections", ***Eng. Struct***., Vol. 30, (2008), 2566-2579.
10. Chen, W.F. and Lui, E.M., "Stability design of steel frame", Florida, Boca Raton, CRC Press, (1991).
11. Hayalioglu, M.S. and Degertekin, S.O., "Minimum cost design of steel frames with semi-rigid connections and column bases via genetic optimization", ***Comput. Struct***., Vol. 83, (2005), 1849-1863.
12. Kameshki, E.S. and Saka, M.P., "Genetic algorithm based optimum design of nonlinear planar steel frames with various semirigid connections", ***J. Constr Steel Res***., Vol. 59, (2003), 109-134.
13. Dhillon, B.S. and O'Malley III, J.W., "Interactive design of semirigid steel frames", ***J. Struct. Eng. ASCE***., Vol. 125 (1999) 556-564.
14. CSA, "Steel structures (Limit States Design) ", CAN/CSA-S16-01, Toronto, Ontario, Canadian Standards Association, (2001).
15. CEN, "Eurocode 3: Design of steel structures", European Committee for Standardization, (1992).
16. AISC, "Steel construction manual", 13th ed., Chicago, American Institute of Steel Construction, (2006).
17. Zhou, Z.H. and Chan, S.L., "Self-equilibrating element for second-order analysis of semirigid jointed frames", ***J. Eng. Mech. ASCE***., Vol. 121, (1995), 896-902.
18. Xu, L., "Second-order analysis for semi-rigid steel frame design", ***Can. J. Civ. Eng***., Vol. 28, (2001), 59-76.
19. Sekulovic, M. and Salatic, R., "Nonlinear analysis of frames with flexible connections", ***Comput. Struct***., Vol. 79, (2001), 1097-1107.
20. Liu, Y., Xu, L. and Grierson, D.E., "Compound-element modeling accounting for semi-rigid connections and member plasticity", ***Eng. Struct***., Vol. 30, (2008), 1292-1307.
21. Liu, Y., "Hybrid-member stiffness matrix accounting for geometrical nonlinearity and member inelasticity in semi-rigid frameworks", ***Eng. Struct***., Vol. 31, (2009) 2880-2895.
22. G.R. Monforton, T.S. Wu, "Matrix analysis of semi-rigidly connected steel frames", ***J. Struct. Div. ASCE***., Vol. 89, (1963), 13-42.
23. Rezaiee-Pajand, M. and Alamatian, J., "Implicit higher-order accuracy method for numerical integration in dynamic analysis", ***J. Struct. Eng. ASCE***., Vol. 134, (2008), 973-985.
24. Newmark, N.M., "A method of computation for structural dynamics", ***J. Eng. Mech. Div. ASCE***., Vol. 85, (1959), 67-94.
25. Wilson, E.L., Farhoomand, I. and Bathe, K.J., "Nonlinear dynamic analysis of complex structures", ***Earthquake Eng Struct Dyn***., Vol. 1, (1973), 241-252.
26. Rezaiee-Pajand, M. and Alamatian, J., "Nonlinear dynamic analysis by Dynamic Relaxation method", ***Struct. Eng. Mech***., Vol.28 (2008), 549-570.
27. Chan, S.L. and Chui, P.T., "Nonlinear static and cyclic analysis of steel frames with semi-rigid connections", Amsterdam, Elsevier Science, (2000).
28. Chen, W.F., "Practical analysis for semi-rigid frame design", Singapore, World Scientific, (2000).
29. Raftoyiannis, I.G., "The effect of semi-rigid joints and an elastic bracing system on the buckling load of simple rectangular steel frames", ***J. Constr. Steel Res***., Vol. 61, (2005), 1205-1225.
30. Sekulovic, M., Salatic, R. and Nefovska, M., "Dynamic analysis of steel frames with flexible connections", ***Comput. Struct***., Vol. 80, (2002), 935-955.
31. Morris, G., Huang, J. and Scerbo, M., "Accounting for connection behaviour in steel frame design", ***Can. J. Civ. Eng***., Vol. 22, (1995), 955-969.